Pu$_2$O$_3$ and the plutonium hydriding process

L.N. Dinh *, J.M. Haschke, C.K. Saw, P.G. Allen, W. McLean II

Lawrence Livermore National Laboratory, Livermore, CA 94551, USA

ARTICLE INFO

ABSTRACT

The role of cubic Pu$_2$O$_3$ in the corrosion of PuO$_2$-coated Pu by H$_2$ was investigated. Experiments were conducted to demonstrate that nucleation of hydriding is promoted by formation of Pu$_2$O$_3$ sites in the oxide layer. The nucleation mechanism based on diffusion of hydrogen through the PuO$_2$ layer was evaluated and an alternative mechanism based on formation of catalytic Pu$_2$O$_3$ sites via the Pu–PuO$_2$ reaction is proposed. The possibility of active participation of other impurities and inclusions in the dioxide is also discussed.

Published by Elsevier B.V.

1. Introduction

An adequate understanding of plutonium corrosion is needed to ensure that personnel and the environment are protected during handling and storage of Pu metal. Formation of plutonium hydride is of concern because it is pyrophoric and catalyzes a violent reaction of Pu metal with O$_2$ and N$_2$ upon exposure to air [1]. Although heat generation poses a significant hazard, a larger safety concern arises because the reactions transform non-dispersible metal into products with large mass fractions of dispersible and respirable plutonium-containing particles.

Hydrogen corrosion of oxide-coated plutonium follows a nucleation and growth pattern with wildly different induction times for the nucleation stage of reaction [2,3]. The near surface region of oxidized Pu is reported to consist of a series of oxides starting on the outside with PuO$_2$ in varying thicknesses (depending on the fabrication routes) followed by a layer of Pu$_2$O$_3$ or Pu$_2$O$_3$ + PuO$_{0.5}$ C$_{0.4}$, and finally Pu metal [1,4]. Larson reported a series of ellipsometric measurements and found typical surfaces to have an oxide thickness on the order of a few hundred to a few thousand Angstroms [5]. In a later study, Haschke reported that the oxide layer becomes unstable due to build-up of stress from the lattice mismatch between oxide and metal at thickness on the order of a few micrometers [1]. Therefore, typical oxide layers are most likely within these limits.

Nucleation is an essential and perplexing reaction step that merits further investigation. Appearance of an induction period is widely attributed to slow diffusion of hydrogen through the PuO$_2$ layer on Pu surfaces [3,6–9]. Accumulation of hydrogen at the oxide–metal interface then results in localized hydriding that expands and ruptures the overlying oxide. In this report, techniques

to mechanically or chemically disturb the surface oxide were employed and resulted in drastic reduction of induction time as well as a significant increase in reaction rates. This implies that the state of the oxide is of great importance in the initiation of corrosion in Pu. A hydriding corrosion process, in which hydriding can be catalyzed by the cubic Pu$_2$O$_3$ phase formed under non-oxidizing conditions [10], is then suggested.

2. Surface chemistry and nucleation mechanisms

Onset of hydriding is strongly influenced by the chemistry of preexisting corrosion products on the plutonium surface. In air at typical storage temperature, PuO$_2$ is the dominant surface phase, but thermodynamic constraints require that a layer of Pu$_2$O$_3$ must exist at the oxide interface [1,4]. The thickness of the oxide layer, ranging from a few nanometers on freshly cleaned surface to the micrometer range on extensively oxidized metal, is an important factor in controlling the reaction kinetics. Oxidation of Pu with a thin oxide layer is described by parabolic kinetics, implying that the rate is initially controlled by diffusion of oxygen through the PuO$_2$ layer of progressively increasing thickness [1,10]. A transition to linear (constant oxidation rate) kinetics after extensive oxidation coincides with fracture of the oxide and maintenance of a constant average oxide thickness by continuous spallation and re-oxidation [10,11]. As shown schematically in Fig. 1a, the PuO$_2$ thickness on extensively oxidized metal varies markedly from a constant thickness. Chemical properties of the oxide vary sharply with temperature and oxygen activity of the storage atmosphere [1]. Under non-oxidizing conditions, PuO$_2$ is transformed to cubic Pu$_2$O$_3$ by the temperature dependent autoreduction reaction with Pu [1,4].

As outlined above, two possible nucleation mechanisms merit detailed consideration: (1) diffusion of hydrogen through the dioxide surface layer, followed by formation of autocatalytic hydride

* Corresponding author. Address: Lawrence Livermore National Laboratory, 7000 East Avenue, Mail Stop: L091, Livermore, CA 94551, USA. Tel.: +1 925 422 4271.
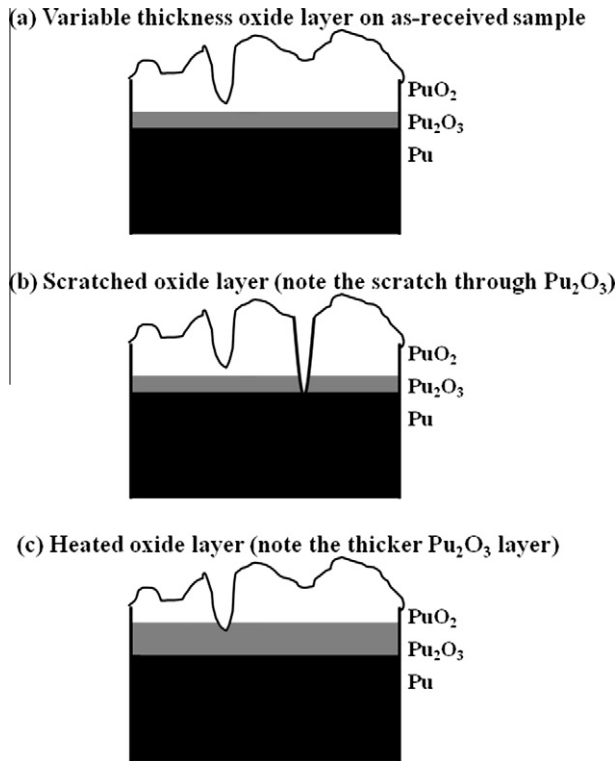*E-mail address:* Dinh1@llnl.gov (L.N. Dinh).

Fig. 1. Schematic description of oxide surface layers on extensively oxidized Pu: (a) variable thickness PuO_2 layer with a thin interfacial Pu_2O_3 layer on as-received sample, (b) penetration of the oxide layers by a deep scratch, (c) expansion of the Pu_2O_3 layer by heating in vacuum.

Fig. 2. Solubility of hydrogen in uranium dioxide and plutonium metal as a function of temperature. Solubilities at 10 bar H_2 pressures [14] are shown for single crystal (SC) UO_2 (solid triangles), polycrystalline (PC) $UO_{2.0}$ (open triangles), polycrystalline $UO_{2.065}$ (solid squares), and polycrystalline $UO_{1.976}$ (open squares). Solubilities at the equilibrium phase boundaries of Pu [16] are shown for unalloyed Pu (solid circles) and delta-stabilized alloy containing 2 wt.% Ga (open circles).

sites at the oxide-metal interface, and (2) penetration of the PuO_2 layer by mechanical or chemical methods, followed by catalyzed formation of hydride beneath Pu_2O_3 sites. Evaluation of these mechanisms is based on thermodynamic assessment of each concept. Application of this approach leads to immediate rejection of a third concept based on formation of OH^-. Since PuO_2 is the only oxygen source in the chemical system, formation of hydroxide must proceed by hydrogen reduction of the dioxide: $5PuO_2 + 2H_2 \rightarrow 2Pu_2O_3 + Pu(OH)_4$. Thermodynamic data [12,13] show that the change in Gibb free energy for this reaction at standard temperature and pressure, ΔG°, is +99 kJ/mol of OH^-.

Thermodynamic evaluation of the mechanism based on hydrogen diffusion is constrained by lack of hydrogen solubility data for PuO_2. However, uranium dioxide is a reasonable surrogate because structural and thermodynamic properties of UO_2 and PuO_2 correspond closely. Solubilities in the stoichiometric dioxides depend on hydrogen accommodation in fluorite type lattices with molar volumes that differ by only 3.8%. Measured solubilities of hydrogen in UO_2 at 10 bar H_2 pressure [14] are shown as a function of temperature in Fig. 2. Wheeler reported much higher solubilities of hydrogen in single crystal dioxide [15], but attributed the high solubilities to unspecified high level of defects in his samples. Hydrogen trapped at defective sites have been observed during hydrogen desorption by the existence of multiple desorption peaks as temperature was ramped upward [14,15]. The higher solubility in polycrystalline UO_2 relative to that of single crystal UO_2 is consistent with a higher level of grain boundary defects and impurities in the commercially supplied oxide used in the study. Agreement of the results for hyperstoichiometric $UO_{2.065}$ at 1327 °C with those for stoichiometric $U_{2.0}$ implies that solubility is insensitive to the presence of interstitial oxygen. In contrast, the solubility in $UO_{1.976}$ is 20 fold higher than in the dioxide and infers that dissolution of hydrogen is promoted by anion vacancies in the oxide lat-
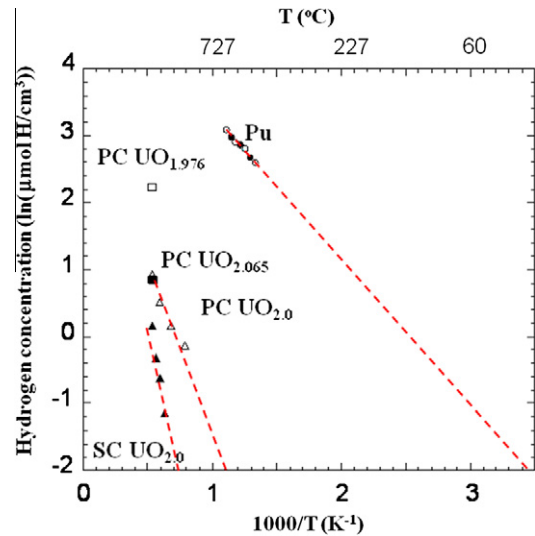
tice. Proportionality of solubility to the square root of the H_2 pressure at constant temperature [14] implies that dissolution proceeds by dissociation of H_2 at the gas–oxide interface and accommodation as an atomic species (H^-, H, H^+) in the lattice.

Formation of hydride nucleation sites via a hydrogen diffusion mechanism is possible only if the hydrogen activity at the oxide-metal interface exceeds that for hydrogen-saturated plutonium at the reaction temperature. The interface concentration cannot be greater than the solubility of hydrogen in the dioxide. The concentration of dissolved hydrogen in polycrystalline $UO_{2.0}$ at 10 bar H_2 pressure is too low by many orders of magnitude when compared with phase-boundary hydrogen concentration for unalloyed Pu and delta-stabilized Ga alloy [16] as seen in Fig. 2. Results of an earlier equilibrium study of the Pu–H system [17] show that phase boundary concentrations at 500–600 °C exceed the extrapolated oxide solubility by an additional factor of 10. The solubility curve for dioxide and metal apparently do not converge at low temperature and application of a H_2 pressure greater than 10^8 bar would be required to form hydride. Neither the magnitude of uncertainty associated with oxide purity nor the error introduced by use of surrogate solubility data for PuO_2 can be quantified, but validity of the concept based on diffusion of hydrogen through an ideal (defect-free) dioxide layer is doubtful. The existence of multiple hydrogen desorption peaks as temperature was increased implies that hydrogen transport in the dioxide is not a simple/ideal diffusion process [14,15].

Studies show that the hydriding kinetics of Pu are sensitive to the composition of surface oxide [1,10,18] and suggest the possibility of a nucleation mechanism based on chemical alteration of the oxide layer by spontaneous formation of Pu_2O_3 via the PuO_2–Pu reaction. Cubic Pu_2O_3 is a substoichiometric fluorite-related oxide with an anion vacancy concentration (25%) much greater than that of $UO_{1.976}$ (0.6%) (Fig. 2). Unlike PuO_2 that throttles the hydriding rate of Pu, cubic Pu_2O_3 catalyzes the reaction at a rate equal to that of the autocatalytic hydride [10,18]. This high reactivity of Pu_2O_3 coated metal implies that the highly defective oxide is capable of accommodating and transporting a large amount of hydrogen. In the absence of an oxygen source that maintains the dioxide surface (Fig. 1a), autoreduction of PuO_2 by Pu progressively

transforms the surface to Pu_2O_3 via the reaction: $Pu + 3PuO_2 \rightarrow 2Pu_2O_3$ ($\Delta G° = -83.3$ kJ/mol of Pu_2O_3) [12]. This thermodynamically favorable reaction proceeds as oxygen diffuses out of the PuO_2 lattice, leaving cubic Pu_2O_3 in place of PuO_2 and forming additional sesquioxide at the oxide-metal interface [4]. This process is slow at 22 °C [19], but readily transforms PuO_2 at and above 200 °C [19]. As a function of time and temperature, the reaction progressively increases the thickness of the Pu_2O_3 layer and ultimately penetrates the PuO_2 layer at the thinnest point (Fig. 1c). Catalyzed hydride formation beneath the site results in fracture of the oxide over-layer and continuing autocatalyzed reaction at the site.

In early hydriding studies, workers observed that induction periods were consistently shortened by scribing oxide-coated surfaces and by heating oxide-coated samples prior to hydrogen exposure [2]. Experiments employing these enhancement techniques are complementary and provide a basis for further characterization of the nucleation process. Scribing of a PuO_2-coated surface as shown schematically in Fig. 1b should promote reaction along the scratch by thinning the PuO_2 layer or by exposing interfacial Pu_2O_3, but does not permit discrimination between the hydrogen diffusion and Pu_2O_3 concepts. As indicated in Fig. 1c, moderately heating a PuO_2-coated sample in low vacuum does not significantly change the oxide thickness and the nucleation process should remain unaltered if reaction proceeds via hydrogen diffusion. In contrast, hydriding at numerous sites like that shown in Fig. 1c is anticipated if nucleation is catalyzed by Pu_2O_3.

3. Experimental methods

Experiments to investigate the nucleation kinetics of the Pu–H_2 reaction were made by pressure volume temperature (PVT) method with samples (16 mm diameter × 1 mm thick) of Ga-stabilized delta-phase plutonium alloy. The circular samples were machined from a rolled sheet that had been milled. The cut samples were rinsed with ethanol and then exposed to air until an amber-colored surface layer of PuO_2 had formed. Prior to experiment, each Pu sample was mounted in an aluminum sample holder fitted with an indium o-ring that was compressed against one surface of the sample and confined the reaction of H_2 to a 13 mm diameter visible surface.

Hydriding experiments were conducted using samples with three different preparative histories corresponding to the diagrams in Fig. 1: (a) as received, (b) with a deep scratch made in the oxide surface layer by a diamond tipped scriber in a dry argon purged glove box, and (c) after heating at 110 °C in vacuum for 2 days and cooling to room temperature. For experiments associated with Fig. 1b, a deep scratch was made near the center of the sample. For experiments associated with Fig. 1c, temperature during heating was limited to 110 °C to avoid softening and failure of the indium seals in the sample holders. The length of the heating period was selected in an effort to appropriately increase the thickness of the Pu_2O_3 interface layer so that only the thinnest areas in the oxide layer would be penetrated (Fig. 1c).

Mounted samples were placed in volume-calibrated stainless steel reaction chambers that were then evacuated to a base pressure of 10^{-2} Pa with an oil-free scroll pump. Each test was initiated by rapid pressurization of the reaction chamber with 7 mmol of research grade H_2. The appearance and growth of hydride sites were recorded using a video camera with a view of the sample surface through a sapphire window. Consumption of hydrogen was measured as a function of time (t) by PVT method at room temperature (~27 °C). Pressures were measured with quartz oscillator gauges (ParoScientific model 6000-200 A). Hydriding rate were calculated from measured ΔP and Δt increments using the ideal gas law. The

PuO_2–Pu autoreduction reaction is well documented by in situ XPS [19] and XRD [20] measurements at temperatures bracketing 110 °C, and its occurrence in this study is expected, but not verified.

4. Results and discussion

Observations of the Pu–H_2 reaction [21] are consistent with early work that identified a sequence of reaction steps and with reports that the hydriding rate is determined by surface properties. Video and PVT data for as-received samples show induction periods (100–150 s) followed by acceleration of the reaction rate. Induction periods are not observed for scratched or heated samples. Relative to the acceleration rate of as-received samples, scratching produced a 2 fold enhancement and heating caused the rate to increase by a factor of 5–6.

A qualitative, but informative, perspective on early stages of hydriding is gained from photographs recorded from the video camera (Fig. 3). Note that the white regions in columns (a) and (b) were due to light reflection. The absence of reflected light from the heated sample at 0% shown in column (c) was due to the position of the illumination source, not a change in surface reflectivity from heating. At 0% reaction, differences are not evident in the samples, except for the scratch on the sample shown in column (b). The effects of surface alteration are indicated by three properties of samples at 30% reaction: the concentration, size distribution, and location of nucleation sites.

Examination of photographs for the as-received sample at 30% shows a modest number of hydride sites that cover a relatively small fraction of the surface. The sizes of the sites vary substantially with a few relatively large sites (~1 mm diameter) that were first to nucleate and account for most (>90%) of the consumed H_2. A distribution of sites (~50) with progressively smaller dimensions apparently formed in succession over time. Video data show that the initial sites formed spontaneously, and that additional sites appearing later in time also nucleated after impingement of spallation-ejected hydride particles on the oxide-coated sample. Besides catalyzing the $H_2 \rightarrow 2H$ reaction, these hydride particles were thermally hot, chemically reactive, and were clearly responsible for the hydriding at the locations of their landing. Formation of Pu_2O_3 and H_2 by the reaction: $PuH_2 + 3PuO_2 \rightarrow 2Pu_2O_3 + H_2$ ($\Delta G° = -35.9$ kJ/mol of PuH_2) [13,22] is energetically favorable. The rate of PuO_2 reduction by Pu is promoted because of the temperature increase generated by this reaction and by the heat content of the ejected hydride particles. Formation of a catalytic Pu_2O_3 site via these reactions accounted for the observations, but was not experimentally verified.

The extent of particle ejection during hydriding is shown (Fig. 3) by examination of the sample-holder surface surrounding the sample. The photographs show that the surface of the sample holder after 30% reaction is not noticeably different than at 0%. Examination of the surface of the sample holder after 100% reaction shows numerous hydride particles. The potential impact of particle ejection on nucleation was evident because nucleation sites covered the Pu sample surface after reaction was complete. The video record shows that the frequency of hydride particle ejection became increasingly important as reaction proceeded. The observed concentration and size distributions of sites at 30% reaction are an apparent consequence of the inherent nucleation process, but occurrence of satellite nucleation around initial sites due to hydride particles ejection mentioned above cannot be excluded.

An intriguing phenomenon was encountered during review of the video record: ejected hydride particles on the Pu sample surface and the surrounding aluminum holder remained mobile and appeared to bounce up and down. This behavior may be related
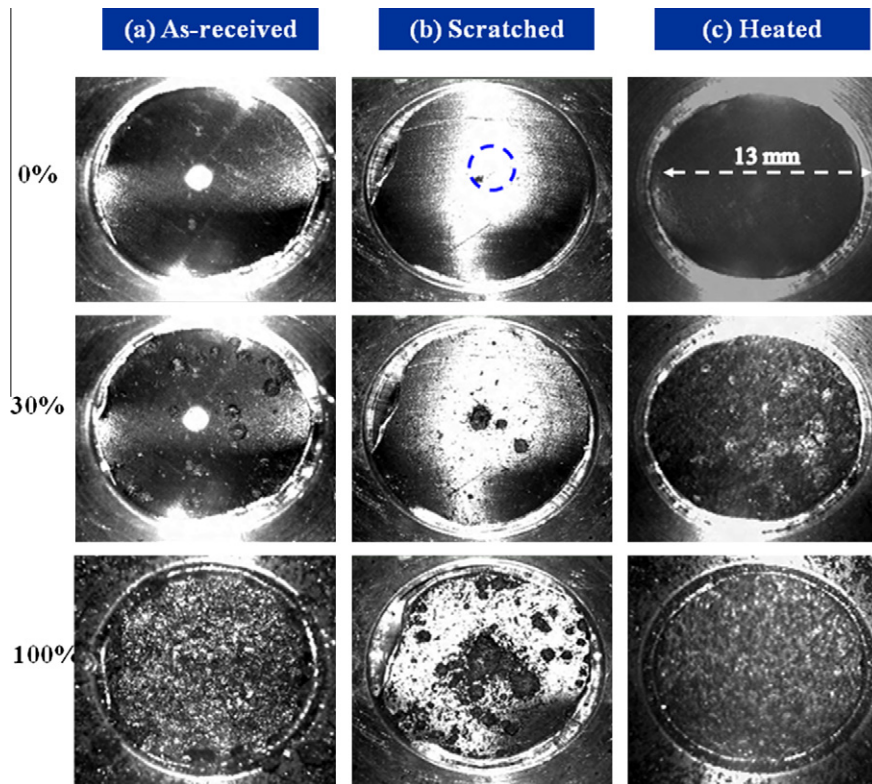
Fig. 3. Photographs showing the effects of scratching and heating on the Pu–H$_2$ reaction. Each column shows the sample surface immediately before H$_2$ was added (0%), at 30% consumption of H$_2$, and at 100% consumption of H$_2$. Note that 30% and 100% reaction were reached at different points in time after the addition of H$_2$. Bright surface areas were caused by reflection of light from the illumination source. The dashed circle in column (b) at 0% is inserted to identify the scratch.

to continuing reaction of low-composition hydride particles with hydrogen to form PuH$_{2+x}$ ($x \leqslant 1$).

Behavior of scratched samples (Fig. 3b) was noticeably different than that of as-received samples. Hydriding consistently and immediately nucleated at the scratch. Thereafter, reaction proceeded to penetrate deep into and through the metal at that site without extensive hydride particle ejection or nucleation of additional sites.

In some ways, hydriding of previously vacuum-heated samples was similar to that of as-received metal (Fig. 3c), but proceeded at a relatively rapid rate. As shown by the photograph at 30% reaction, the surface was almost completely covered by numerous small sites. In contrast, the same amount of H$_2$ reacted with as-received samples over a longer time period at few large sites. Both, as-received and previously vacuum-heated samples ultimately hydrided with extensive ejection of hydride particles and were indistinguishable after 100% reaction. Vacuum heating did not appreciably alter the oxide thickness, but apparently activated a large numbers of nucleation sites on the oxide-coated Pu by exposing Pu$_2$O$_3$ to direct contact with H$_2$ where the oxide was thinnest as seen in Fig. 1c.

Results obtained from PVT measurements of hydriding rates are consistent with video observation and provide additional insight into the nucleation process. In Fig. 4, the hydriding rates for the three sample types are shown as a function of time. The rate-time curves for as-received and vacuum-heated samples exhibit upward curvature over time, whereas the somewhat erratic results for scratched samples are essentially linear. Acceleration of the rate was constant for scratched samples because the formation of additional sites was limited as mentioned above. The upward curvature for the rate-time curves of as-received and vacuum-heated samples is consistent with camera video record evidence of the forma-
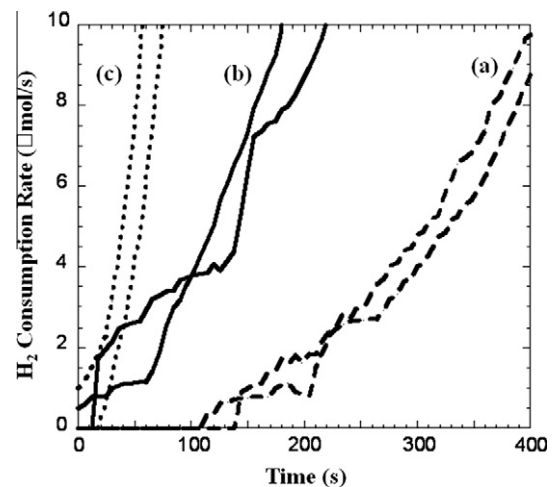

Fig. 4. Time dependence of the hydriding rates: (a) as-received samples (dashed), (b) scratched samples (solid), and (c) heated samples (dotted).

tion of significant additional nucleation sites over time, a change that progressively accelerated the reaction as hydriding proceeded.

The absence of induction periods for scratched and heated samples is important, but an especially significant result is the observation of non-zero initial rates for many of these samples (Fig. 4). The hydriding rate of Pu is proportional to the area of reactive hydride on the surface [2]. If reaction of a Pu sample is stopped by removing the H$_2$ and then resumed by replacing the gas, the reaction rate is precisely reestablished as if the interruption had never occurred [2]. Therefore, appearance of a finite rate at zero time implies that

one or more catalytic site were present before H_2 was introduced. The observed rate must have been catalyzed by another phase that was formed by heating or scratching. The results strongly support a nucleation mechanism based on the formation of Pu_2O_3.

5. Conclusions

Thermodynamic evaluation of the nucleation model based on diffusion of hydrogen through the dioxide layer on plutonium shows that the solubility of hydrogen in PuO_2 at practical temperatures and pressures is orders of magnitude below that required for nucleation of plutonium hydride reaction sites. Solubility of H_2 in UO_2 is noticeably increased by formation of anion vacancies and one might conclude that the solubility in highly defective Pu_2O_3 might be sufficient to form hydride. The formation of such a defective oxide is the basis for the alternative hydriding mechanism proposed in this report. That concept is based on the diffusion of oxygen out of the fluorite-type PuO_2 layer and reaction with Pu to form Pu_2O_3, a highly defective oxide and known catalyst for the Pu–H_2 reaction.

Tests designed to chemically and mechanically alter the dioxide surface on Pu and to determine the effect on nucleation show that induction periods are consistently eliminated at conditions that produce Pu_2O_3 sites. The presence of catalytic Pu_2O_3 is consistent with observation of measurable hydriding rates at zero time and of higher hydriding rates for scratched samples and vacuum-heated samples in comparison with as-received Pu samples.

An especially perplexing aspect of plutonium chemistry is the unpredictability of induction. Reaction nucleates immediately in some cases but fails to initiate over long periods of time in other cases at duplicate conditions. Local spallation of oxide from PuO_2 coated metal is a well-known process that relieves the stress between the low-density surface oxide and the high-density plutonium. Spallation forms seemingly random local areas with a thin dioxide over-layer. The reaction of Pu with PuO_2 to form catalytic Pu_2O_3 sites at locals with thin oxide is crucial for the nucleation of hydriding sites. The relative short induction time of 100–150 s observed for the nucleation of quite a few seemingly random sites on as-received Pu samples points to the fact that the native PuO_2 layer formed on these Pu samples is far from being an ideal (defect-free) dioxide. Other defects in the dioxide such as micro-cracks, short-range or local oxygen vacancies, or some forms of impurity inclusions that promote hydriding are also expected to increase the solubility of hydrogen in the dioxide and to serve as conduit for hydrogen transport to the oxide-metal interface. Surely, the properties of such defects are different than those of Pu_2O_3 but the possibility of their involvement in seemingly random appearance of nucleation sites on as-received PuO_2-coated plutonium cannot be ignored.

Experimental efforts in measuring the temperature profile of the Pu sample during hydriding reaction, perhaps with the help of a pyrometer camera, are planned for the near future. These temperature profiles will be combined with hydriding kinetic data to arrive at a quantitative nucleation and growth model.

References

[1] J.M. Haschke, J.L. Stakebake, in: L.R. Morss, N.M. Edelstein, J. Fuger, (Eds.), Chemistry of the Actinide and Transuranium Elements, vol. 5, Springer, Dordrecht, 2006, pp. 3199–3272 (Chapter 29).
[2] J.M. Haschke, Synthesis of lanthanide and actinide compounds, in: G. Meyer, L.R. Morss (Eds.), Kluwer Academic Publishers, 2001, pp. 1–53.
[3] G.W. McGillivray, J.P. Knowles, I.M. Findlay, M.J. Dawes, J. Nucl. Mater. 385 (2009) 212.
[4] H.G.G. Flores, D.L. Pugmire, Mater. Sci. Eng. 9 (2010) 012038.
[5] D.T. Larson, D.L. Cash, J. Phys. Chem. 73 (1969) 2814.
[6] J. Bloch, E. Swissa, M.H. Mintz, Z. Phys. Chem. Neue Folge 1964 (1989) 1193.
[7] J. Bloch, M.H. Mintz, J. Less Common Met. 166 (1990) 241.
[8] D. Cohen, Y. Zeiri, M.H. Mintz, J. Alloys Compd. 184 (1992) 11.
[9] J. Glasscott, AWE Discov. 6 (2003) 6.
[10] J.M. Haschke, T.H. Allen, L.A. Morales, Los Alamos Sci 26 (2000) 252.
[11] J.R. Kirkpatrick, J.B. Condon, J. Less Common Met. 172–174 (1991) 124.
[12] R. Lemire, J. Fuger, H. Nitsche, M. Rand, P. Potter, J. Rydberg, K. Spahiu, J. Sullivan, W. Ullman, P. Vitorage, H. Wanner, Chemical Thermodynamics of Neptunium and Plutonium, Elsevier, Amsterdam, 2001. pp. 55–64.
[13] D. Langmuir, Aqueous Environmental Geochemistry, Prentice Hall, 1997. pp. 557.
[14] D.F. Sherman, D.R. Olander, J. Nucl. Mater. 166 (1989) 307.
[15] V.J. Wheeler, J. Nucl. Mater. 40 (1971) 189.
[16] T.H. Allen, The Solubility of Hydrogen in Plutonium in the Temperature Range 475–826 Degree Centigrade, Thesis, University of Colorado at Denver 1991.
[17] R.N.R. Mulford, G.E. Sturdy, J. Am. Chem. Soc. 77 (1955) 3449.
[18] J.M. Haschke, T.H. Allen, J. Alloys Compd. 320 (2000) 58.
[19] D.T. Larson, J.M. Haschke, Inorg. Chem. 20 (1981) 1945.
[20] K. Terada, R.L. Meisel, M.R. Dringman, J. Nucl. Mater. 30 (1969) 340.
[21] K. Balasubramanian, T.E. Felter, T. Anklam, T.W. Trelenberg, W. McLean II, J. Alloys Compd. 444–445 (2007) 447.
[22] H.E. Flotow, J.M. Haschke, S. Yamauchi, Int. Atom. Energy Agency (1984) 49.